Dynamics of Celestial Bodies, 51 - 65 *Invited paper*

LOCAL AND GLOBAL DIFFUSION ALONG RESONANT LINES IN CONTINUOUS AND DISCRETE QUASI–INTEGRABLE DYNAMICAL SYSTEMS

C. FROESCHLÉ[1], M. GUZZO[2] and E. LEGA[1]

[1] *CNRS UMR6202, Observatoire de la Côte d'Azur, Bv. de l'Observatoire, B.P. 4229, 06304 Nice cedex 4, France*

[2] *Università degli Studi di Padova, Dipartimento di Matematica Pura ed Applicata via Trieste 63, 35121 Padova, Italy*

Abstract. The characterization of diffusion of orbits in Hamiltonian quasi-integrable systems is a relevant topic in dynamics. For quasi-integrable Hamiltonian systems a possible model for global diffusion, valid for perturbations larger than a critical value, was given by Chirikov; while for smaller perturbations the Nekhoroshev theorem leaves the possibility of exponentially slow diffusion on a subset of the possible dynamical states with peculiar topology, the so-called Arnold's web. We have studied this problem using a numerical approach. This paper contains a review of papers that we published concerning the numerical detection of Arnold's diffusion in continuous and discrete quasi–integrable dynamical system.

1. INTRODUCTION

The characterization of mechanisms for diffusion of orbits in quasi–integrable Hamiltonian systems and symplectic maps is a relevant topic for many fields of physics, such as celestial mechanics, dynamical astronomy, statistical physics, plasma physics and particle accelerators.

In 1979 Chirikov (Chirikov 1979) described a possible model for global drift valid when the perturbation is greater than some critical value. Chirikov's model has so far been successfully used to describe diffusion in systems from different fields of physics (see for example Morbidelli 2002). One of the reasons of the broad detection of the Chirikov's diffusion is that its typical times fall within the simulation abilities of modern computers as far back as the seventies. For smaller perturbations the systems fall within the range of celebrated perturbation theories such as KAM (Kolmogorov 1954,Arnold 1963, Moser 1958) and Nekhoroshev theorems (Nekhoroshev 1977), which leave the possibility for a drift only on a subset of the possible dynamical states with peculiar topology, the so–called Arnold web, and force diffusion times to be at least exponentially long with an inverse power of the norm of the perturbation. The theoretical possibility of drift in slightly perturbed systems has been first

shown in 1964 by Arnold (Arnold 1964) for a specific system, and is commonly called Arnold diffusion.

Being interested to applications to specific systems, and in particular to systems of interest for physics, we have used a numerical approach which, avoiding theoretical difficulties, measures directly the quantitative features of eventual long term diffusion. In 2003 we numerically detected a very slow local diffusion confined to the Arnold web (Lega et al. 2003) in a model perturbed system satisfying both the KAM and Nekhoroshev hypothesis. In that work we have numerically measured a diffusion coefficient showing that it decreases faster than a power law of the perturbing parameter and in agreement with the Nekhoroshev theorem.

The Arnold's mechanism is related to a specific "ad hoc" model and the generalization of the mechanism to generic quasi-integrable systems is still an open problem. One of the main difficulties is the so-called "large gap" problem (LGP hereafter), which is related to low order resonance crossings. A new approach to solve the LGP has been recently introduced (Delshams et al. 2003) to prove the existence of diffusion in the so-called a priori unstable systems. Instead, the LGP has not been yet solved for generic quasi-integrable systems.

Therefore, we found it interesting to explore the possibility for orbits of a generic system to globally diffuse, i.e. to explore macroscopic regions of the space, in a model problem in which the "gap problem" is present. In 2005 we have provided numerical evidence both on quasi–integrable Hamiltonian systems and symplectic maps of a relevant phenomenon of global diffusion of orbits occurring on the Arnold web (Guzzo et al. 2005). More precisely, we have shown that a set of well chosen initial conditions practically explores the whole web and, in the case of maps, the process behaves as a global diffusion.

These results concern systems satisfying the hypothesis of Nekhoroshev theorem (for map see Kuksin 1993, Kuksin and Pöschel 1994, Guzzo 2004).

This paper contains a review of results that we published on this subject and which are more extensively described on (Lega et al. 2007). The paper is organized as follows: In section 2 we give a more general definition of Arnold's diffusion. A brief recall of the numerical tool used to discriminate the dynamics of the orbits is provided in 3. In Section 4 we introduce our model problems. We discuss results about local and global Arnold's diffusion on a suited Hamiltonian model and on maps in 5.

2. A GENERALIZATION OF ARNOLD'S DIFFUSION

Since Arnold model, there have been several generalizations of Arnold diffusion to models more generic than Arnold's one (Arnold 1964), which are motivated not only by mathematical reasons, but also by their significance for physics.

Specifically, concerning the numerical experiments about Arnold diffusion reported in (Tennyson et al. 1979, Lichtenberg and Lieberman 1983, chapter 6, Wood et al. 1990, Lichtenberg and Aswani 1998, Chirikov et al. 1979, Laskar 1993, Efthymiopoulos et al. 1998, Giordano and Cincotta 2004), it appears clearly the existence of different points of view. It is therefore important to define what we consider a generalization of Arnold diffusion. In our papers (Lega et al. 2003, Froeschlé et al. 2005, Guzzo et al. 2005) we considered as Arnold diffusion any exponentially slow diffusion

process occurring on a system which satisfies both the KAM and Nekhoroshev theorems. We find useful to list the definitions we use through the paper as introduced in (Guzzo et al. 2005):

i) *We strictly refer to quasi–integrable systems*, i.e. to Hamiltonian systems with Hamilton functions of the form:

$$H(I,\phi) = h(I) + \epsilon f(I,\phi) \quad , \tag{1}$$

or to symplectic maps:

$$\begin{aligned} I &= I' + \frac{\partial S}{\partial \phi}(I',\phi) \\ \phi' &= \phi + \frac{\partial S}{\partial I}(I',\phi) \end{aligned} \tag{2}$$

where:

$$S(I',\phi) = h(I') + \epsilon f(I',\phi) \tag{3}$$

is a generating function, with action–angle variables (I,ϕ) defined on the open bounded domain $B \times \mathbb{T}^n \subseteq \mathbb{R}^n \times \mathbb{T}^n$.

ii) *The functions h, f are such that the Hamiltonian system (1) and the map (2) satisfy the hypotheses of both KAM and Nekhoroshev theorems (for the KAM and Nekhoroshev theorems for quasi–integrable maps see Kuksin 1993, Kuksin and Pöschel 1994, Guzzo 2004) for suitably small ϵ.* It is sufficient that h and f are analytic and h satisfies a suitable geometric condition, such as quasi–convexity or steepness.

iii) *We consider values of the perturbing parameter ϵ so small that both KAM and Nekhoroshev theorems apply.* This implies that the phase space is almost filled with a set of invariant tori $\mathcal{K}$. Any motion with initial condition on $\mathcal{K}$ is perpetually stable, so that instability can occur only on the complementary set of $\mathcal{K}$, called Arnold web. Moreover, the Nekhoroshev theorem implies that any eventual instability of the actions occurs only on very long times, which increase exponentially with a positive power of $1/\epsilon$.

iv) We will investigate the possibility that the actions I explore macroscopic regions of a given action domain B. By Nekhoroshev theorem this is non trivial and can require very long times as soon as ϵ is small (so that condition (iii) is satisfied and the diameter of the set B is bigger than the local fast oscillations of the actions which are allowed by the theorem). To fix ideas, *we say that a motion $(I(t),\phi(t))$ is 'unstable' if there exists a time t such that:*

$$\|I(t) - I(0)\| \geq \frac{\mathrm{diamB}}{2} \tag{4}$$

It is evident that for small ϵ the existence of unstable motions is not a trivial fact as soon as $\mathrm{diam}B > \sqrt{\epsilon}$.

v) *We say that the N motions $(I^{(j)}(t),\phi^{(j)}(t))$, $j = 1,...N$, diffuse in the action space if the the average evolution of the squared distance of the actions from their initial*

value $(I^{(j)}(0), \phi^{(0)}(t))$ *grows linearly with time.* In other words there exists a constant $D > 0$ such that:

$$S(t) = \frac{1}{N} \sum_{j=1}^{N} [I^{(j)}(t) - I^{(j)}(0)]^2 \sim D\ t \tag{5}$$

for all t.

vi) *Any diffusion of motions for a system satisfying conditions 1, 2 and 3 will be called Arnold diffusion.* For instance, the model studied in (Wood et al. 1990) is not in the form (3) and therefore the slow diffusion detected is not Arnold diffusion in the sense stated above.

3. THE FAST LYAPUNOV INDICATOR

It is well known (see, for example, Morbidelli 2002) that the different diffusion mechanisms which possibly exist in a dynamical system are mainly determined by the geometry of resonances: the Chirikov's one is characterized by resonance overlapping, while Arnold's mechanism for quasi–integrable systems is used when KAM theorem applies, so that the phase space is filled by a large number of invariant tori and the resonances are arranged as a regular web, the so–called Arnold web. A precise numerical detection of the Arnold web (Froeschlé et al. 2000) is possible with the Fast Lyapunov Indicator whose definition (Froeschlé et al. 1997) is related to the Lyapunov exponent theory.

Given an n–dimensional map M, an initial condition $x(0) \in \mathbb{R}^n$, and an initial tangent vector $\vec{v}(0) \in \mathbb{R}^n$ of norm one, let us define the FLI function $FLI(x(0), v(0), T)$, $T > 0$, as:

$$FLI(x(0), v(0), T) = \sup_{0<t\leq T} \log ||v(t)||\,, \tag{6}$$

where $v(t)$ is the tangent vector at time t, which can be computed by the tangent map of M:

$$\left\{ \begin{array}{lcl} x(t+1) & = & M(x(t)) \\ v(t+1) & = & \frac{\partial M}{\partial \vec{x}}(x(t))\, v(t)\,. \end{array} \right. \tag{7}$$

The same definition holds for a continuous flow defined by a differential equation:

$$\dot{x} \quad = \quad F(x) \quad , \quad x \in \mathbb{R}^n \quad , \quad F(x) \in \mathbb{R}^n \tag{8}$$

and the evolution $v(t)$ of tangent vectors is obtained by integrating the linear variational equation of 8.

In the specific case of interest, i.e. the study of quasi-integrable Hamiltonian systems of the form (1) for any initial condition $(I(0), \varphi(0))$ and any initial tangent vector $(v_I(0), v_\varphi(0))$, the FLI at time t is:

$$\log \|(v_I(t), v_\varphi(t))\| \quad . \tag{9}$$

In order to kill non significant fluctuations of (9), in formula (6) we have considered the supremum of the logarithm of the norm of the tangent vector. A running average

could also have been used. Actually, as far as the mathematical development is concerned, we drop these averaging procedures, which however are useful in numerical computations. For $\epsilon = 0$ it is evidently:

$$v_I^0(t) = v_I(0) \quad , \quad v_\phi^0(t) = v_\phi(0) + \frac{\partial^2 h}{\partial^2 I}(I(0))v_I(0)t \quad .$$

If ϵ is small we can estimate the evolution of $||\vec{v}||$ with Hamiltonian perturbation theory. Following (Guzzo et al. 2002) , if the initial condition is on a KAM torus then the norm $||v^\epsilon(t)||$ satisfies:

$$||v^\epsilon(t)|| = \left\| \frac{\partial^2 h}{\partial^2 I}(I(0))v_I(0) \right\| t + \mathcal{O}(\epsilon^\alpha t) + \mathcal{O}(1) \quad , \tag{10}$$

with some $\alpha > 0$. As a consequence, the FLI takes approximately the value of the unperturbed case on all KAM tori. Instead if the initial condition is on a regular resonant motion then it is (Guzzo et al. 2002):

$$||v^\epsilon(t)|| = \|C_\Lambda \Pi_{\Lambda^{ort}} v_I(0)\| \, t + \mathcal{O}(\epsilon^\beta t) + t\mathcal{O}(\rho^2) + \mathcal{O}(\sqrt{\epsilon}t) + \mathcal{O}(\frac{1}{\sqrt{\epsilon}}) \tag{11}$$

with some $\beta > 0$, Λ^{ort} being the linear space orthogonal to an integer lattice Λ (the integer lattice $\Lambda \subseteq Z^n$ defines the resonance, for details see (Guzzo et al. 2002) and C_Λ is a linear operator depending on the resonant lattice Λ and on the initial action $I(0)$.

It is important to remark that the FLI on regular resonant motions is different at order $\mathcal{O}(1)$ from the unperturbed case on regular resonant motions. In fact, the linear operator $C_\Lambda \Pi_{\Lambda^{ort}}$ is different from the Hessian matrix of h at order $\mathcal{O}(1)$, i.e. $C_\Lambda \Pi_{\Lambda^{ort}}$ does not approach $\frac{\partial^2 h}{\partial I^2}$ as ϵ approaches to zero. In this way, we detect the presence of the resonances because the value of the FLI is different from the uniform value assumed on the KAM tori. Finally, for initial conditions on chaotic resonant motions the FLI is higher (since the tangent vectors growth exponentially with time) than the value characterizing KAM tori. As a consequence the resonance structure of the phase space can be detected computing the FLI with the same $v(0)$ and the same time interval t on a grid of regularly spaced initial conditions.

4. THE MODEL PROBLEM

In the following we consider either the quasi-integrable model Hamiltonian studied in (Froeschlé et al. 2000, Guzzo et al. 2002), which is defined by:

$$H = \frac{I_1^2}{2} + \frac{I_2^2}{2} + I_3 + \epsilon \, f \quad , \quad f \; = \; \frac{1}{\cos(\phi_1) + \cos(\phi_2) + \cos(\phi_3) + 3 + c} \quad , \tag{12}$$

where $I_1, I_2, I_3 \in \mathbb{R}$, $\phi_1, \phi_2, \phi_3 \in \mathbb{T}$, $c > 0$, or the quasi–integrable symplectic map studied in (Guzzo et al. 2005, Froeschlé et al. 2005, Guzzo et al. 2006) and defined by:

$$\phi_1' = \phi_1 + I_1 \quad , \quad \phi_2' = \phi_2 + I_2$$

$$I_1' = I_1 + \epsilon \frac{\partial f}{\partial \phi_1}(\phi_1', \phi_2') \quad , \quad I_2' = I_2 + \epsilon \frac{\partial f}{\partial \phi_2}(\phi_1', \phi_2') \tag{13}$$

where $f = 1/(\cos(\phi_1) + \cos(\phi_2) + 2 + c)$, $I_1, I_2 \in \mathbb{R}$, $\phi_1, \phi_2 \in \mathbb{T}$, $c > 0$.

In both cases, when the parameter ϵ is suitably small, the KAM and Nekhoroshev theorems (see Kuksin 1993, Kuksin and Pöschel 1994, Guzzo 2004 for the Nekhoroshev theorem for maps) apply.

The crucial parameters to set in both models are ϵ and the value of constant c appearing in the denominator of the perturbation. In fact, any Fourier harmonic $\epsilon f_k = \epsilon \int f(\phi) \exp(-i \sum_i k_i \phi_i) \mathrm{d}\phi$ of the perturbation f is proportional to ϵ and decreases (asymptotically) exponentially with $c \sum_i |k_i|$. The values of the two parameters must be balanced so that ϵ is smaller than the value for the transition from the KAM regime to the Chirikov regime (determined with numerical methods, see Froeschlé et al. 2000, Guzzo et al. 2002) and the value of c is not too large so that harmonics with large order $\sum_i |k_i|$ produce measurable effects on the finite time scale of our numerical computations. We found suitable values for our experiments $c = 1$ for the Hamiltonian and $c = 2$ for the map.

Finally, we choose such a perturbing functions because the Fourier spectrum of the perturbation contains all harmonics at order ϵ. Any Hamiltonian or map satisfying this requirement would be equivalent while a simple trigonometric potential could not be sufficient to detect numerically the diffusion.

4. 1. THE FLI FOR DETECTING THE GEOMETRY OF RESONANCES

The geometry of resonances of (12) and (13) can be conveniently represented in the two–dimensional plane I_1, I_2. Indeed, each point on this plane individuates univocally the frequency of an unperturbed torus, and the resonances correspond to all the straight lines $k_1 I_1 + k_2 I_2 + k_3 = 0$ for (12), $k_1 I_1 + k_2 I_2 + 2\pi k_3 = 0$ for (13), with $(k_1, k_2, k_3) \in \mathbb{Z}^3 \backslash 0$.

Of course, the set of all resonances is dense on the plane. However, one can expect that resonant orbits surround each resonance line up to a distance which decreases at most as $\sqrt{\epsilon}/|k|^\tau$, with $\tau > 0$ suitable constant.

Fig. 1 shows the FLI chart of Eq. 12 for $t = 4000$ for a grid of 500×500 initial conditions regularly spaced on the action plane for $\epsilon = 0.003$ (the other initial conditions are $\phi_1 = 0$, $\phi_2 = 0$, $\phi_3 = 0$, $I_3 = 1$, the initial tangent vector is $(v_{\phi_1}, v_{\phi_2}, v_{\phi_3}) = (0.5(\sqrt{5} - 1), 1, 1)$ and $(v_{I_1}, v_{I_2}, v_{I_3}) = (1, 1, 1)$).

The FLI is reported with a gray scale: the dark lines correspond to regular resonant motions while the white lines correspond both to chaotic resonant motions or to regular orbits very close to a separatrix. The orbits having a FLI value of about $\log(t)$ constitute the background of KAM tori. It is therefore clear that in Fig. 1 the phase space is mainly filled with KAM tori. Therefore, the FLI chart shown in the figure provide the important indication that for the considered values of ϵ the system is in a regime of validity of the KAM and Nekhoroshev theorems. Also the transition from this regime to the Chirikov one can be detected using the FLI, as we did in (Froeschlé et al. 2000), and the identification of the transition value can be refined (see Guzzo et al. 2002) using a sophisticated analysis of Fourier representations (Guzzo and Benettin 2001).

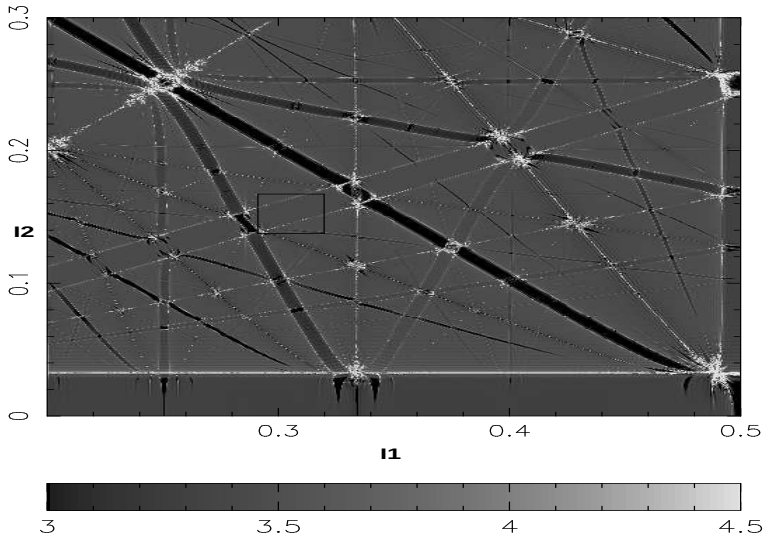

Figure 1: FLI values computed at $t = 4000$ on a grid of 500×500 initial conditions, for Hamiltonian (12), regularly spaced on the action axes I_1 and I_2 for $\epsilon = 0.003$. The other initial conditions are $I_3 = 1$, $\phi_1 = \phi_2 = \phi_3 = 0$, $(v_{\phi_1}, v_{\phi_2}, v_{\phi_3}) = (0.5(\sqrt{5} - 1), 1, 1)$ and $(v_{I_1}, v_{I_2}, v_{I_3}) = (1, 1, 1)$. The gray scale range from black (FLI$\leq$ 3) to white (FLI$\geq$ 4.5). From Lega et al. 2003.

In the following section we focus the attention on a neighborhood of a specific resonance, mainly the $I_1 = 2I_2$ (box in Fig. 1).

5. LOCAL AND GLOBAL ARNOLD'S DIFFUSION

5. 1. LOCAL ARNOLD'S DIFFUSION

In this section we describe the numerical experiment published in (Lega et al. 2003) concerning the Hamiltonian of Eq. 12. Fig. 2 shows enlargements of the FLI chart of the action space around $I_1 = 0.3$, $I_2 = 0.15$ for different values of ϵ. Figs. 2(top) correspond to the box drawn in Fig. 1 for $\epsilon = 0.003$. In these pictures the region between the two white lines is the resonance associated to $I_1 - 2I_2 = 0$, and the two white lines correspond to its hyperbolic border where diffusion is confined. These charts provide us the possibility of choosing initial conditions in this hyperbolic border and to follow their evolution by considering only the points of the orbits which intersect the section of the phase space: $S = \{(I_1, I_2) \in \mathbb{R}^2, I_3 \in \mathbb{R}, \phi_i = 0, i = 1, 2, 3\}$. Of course this can be done numerically by selecting the points satisfying the conditions $\sigma = |\phi_1| + |\phi_2| \leq 0.05$, $\phi_3 = 0$ (reducing the tolerance 0.05 reduces only the number of points on the section, but does not change their diffusion properties). Let us remark, that in such a way we minimize all projection effects and fast quasi-periodic movements. What remains is a very slow drift along the border of the resonance.

We have taken a set of 100 initial conditions in the small interval $0.303 \leq I_1 \leq 0.304$, $0.143 \leq I_2 \leq 0.144$ corresponding to orbits of the FLI charts having FLI values larger than $1.2\log(t)$, $t = 1000$, i.e. corresponding to chaotic orbits in the border of the resonance. Such initial conditions are chosen far from the more stable crossings with other resonances. We have plotted on the FLI charts all the points in the double section described above. Let us remark that such points will appear on both sides of the resonance (in fact the two white lines are connected by an hyperbolic region in the six dimensional phase space).

Fig. 2 (top, left) shows the successive intersections with $\sigma \leq 0.05$, $\phi_3 = 0$, up to a time $t = 10^7$, while Fig. 2 (top, right) extends to $t = 10^8$. Diffusion along the resonant line appears clearly, with speed of the fastest orbits of about 10^{-11}, even for this value of the perturbing parameter, which is one order of magnitude lower than the threshold ϵ_0. We have decreased ϵ and observed diffusion along the resonance with smaller and smaller speed, up to $\epsilon = 0.001$.

Increasing ϵ to 0.007 (Fig. 2 (middle, left) for $t = 10^6$, Fig. 2 (middle, right) for $t = 2.4\,10^7$) the situation does not change, except for the speed of the fastest orbits, which is about 10^{-9}. Instead, for $\epsilon = 0.02$ (Fig. 2 (bottom, left) for $t = 1.6\,10^4$, Fig. 2 (bottom, right) for $t = 5\,10^5$) there is still diffusion along the resonance, but the higher order resonances intersecting the main one become evident and consequently the region of diffusion extends a little also on the direction transversal to the resonance. This happens because the value of the perturbing parameter is approaching the transition value. The speed of the drift is of the order of 10^{-8}. At the transition value we expect that the region of the diffusive orbits almost replaces the region of invariant tori. We remark, that even in this critical situation we still appreciate the diffusion along the resonance on a time $t = 10^5$, with a speed of $4\,10^{-7}$, while for an higher value of $\epsilon = 0.04$ let us emphasize that the set of orbits considered already explores the regions between the resonances in a time $t = 5\,10^4$.

5. 2. MEASURE OF THE DIFFUSION COEFFICIENT

In order to measure the local diffusion along the resonance, it is more efficient to replace the definition of $S(t)$ (given in Eq. 5) with a quantity $\tilde{S}(t)$ which is adapted to the specific resonance, such as:

$$\tilde{S}(t) = \frac{1}{N}\sum_{j=1}^{N}[I_2^{(j)}(t) + 2I_1^{(j)}(t)) - (I_2^{(j)}(0) + 2I_1^{(j)}(0))]^2$$

which corresponds to the average of the Euclidean projection of $(I^{(j)}(t) - I^{(j)}(0))$ along the resonant line. The estimates of D versus $1/\epsilon$ are reported in Fig. 3,left in a logarithmic scale. Clearly, data are not well fitted with a linear regression, which would correspond to a power law $D(\epsilon) = C(1/\epsilon)^m$. Indeed, if we define 3 different sets of data, the first containing the values of D for $1/\epsilon \leq 55$, the second for $62 \leq 1/\epsilon \leq 250$ and the third for $1/\epsilon \geq 330$, and we perform local regression for each set, we find the three different slopes $m_1 = -4.5$, $m_2 = -6.9$ and $m_3 = -8.8$. This is sufficient to exclude a global power law and the changes of slope are in agreement with the expected exponential decrease of D, although an exponential fit of the form $D(\epsilon) = C' \exp(-\kappa/\epsilon)^\alpha$ needs a larger interval of measure in ϵ. Using the map of

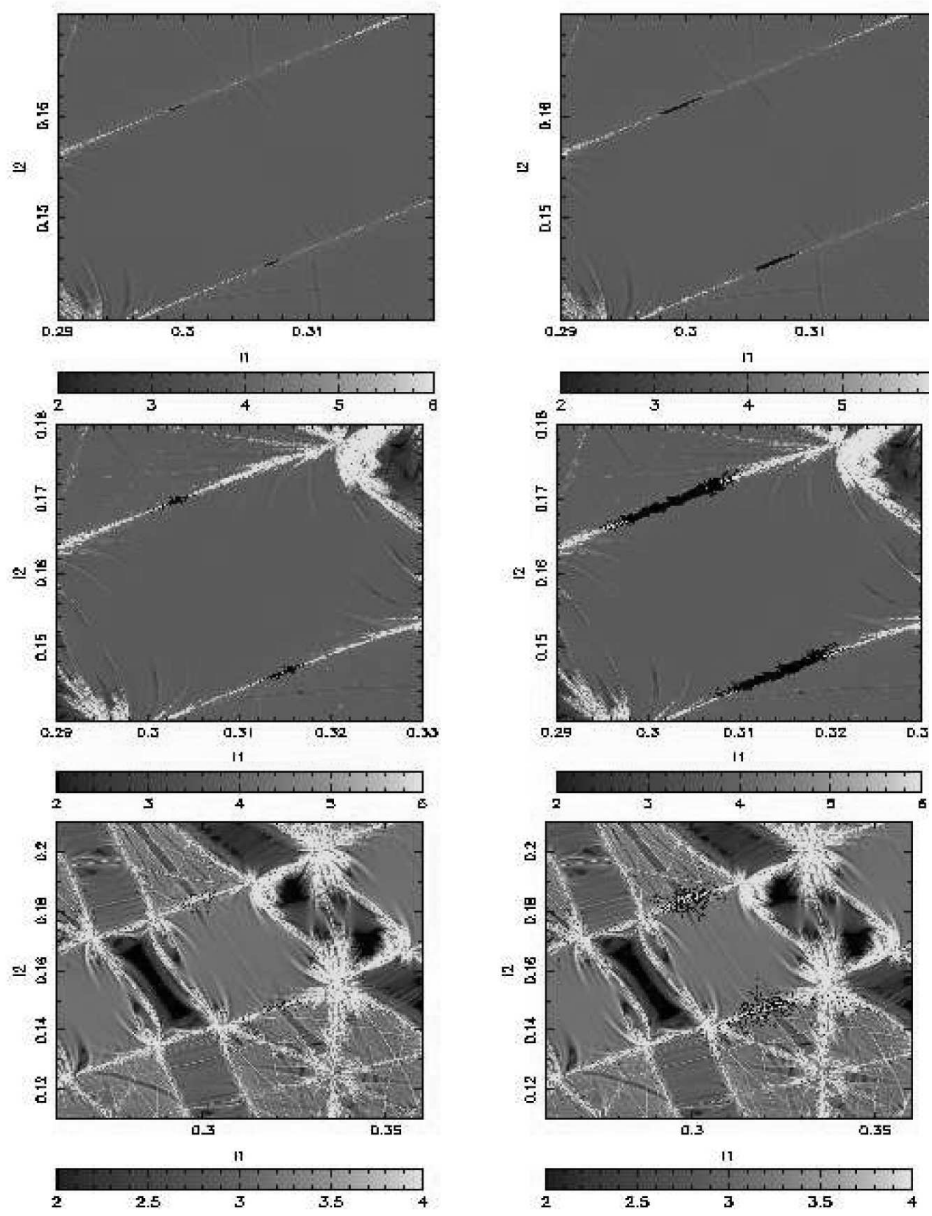

Figure 2: Diffusion along the resonant line $I_1 = 2I_2$ for $\epsilon = 0.003$ (top), $\epsilon = 0.007$ (middle), $\epsilon = 0.02$ (bottom) of a set of 100 initial conditions taken in the hyperbolic border of the resonance in the interval $0.303 < I_1 < 0.304$ and $0.143 < I_2 < 0.144$. The black points are the intersections of the orbits on the double section $|\phi_1| + |\phi_2| \leq 0.05$, $\phi_3 = 0$. The integration times are respectively: $t = 10^7$ (top, left), $t = 10^8$ (top, right), 10^6 (middle, left), $2.4\,10^7$ (middle, right), $1.6\,10^4$ (bottom, left), $5\,10^5$ (bottom, right). The grey scale range from black to white. From Lega et al. 2003.

Eq. 13, we have measured the variation of the local diffusion coefficient for orbits diffusion along the same resonant line $I_1 = 2I_2$. Again, we have defined three sets of data, performing a local regression for each of them, and found three different slopes. The first set contains the values of D for $\ln(1/\epsilon) \leq 0.92$, the second for $1.17 \leq \ln(1/\epsilon) \leq 2.28$ and the third for $\ln(1/\epsilon) \geq 2.43$, and the corresponding slopes are respectively $m_1 = -4.2$, $m_2 = -8.5$ and $m_3 = -13.3$. Such changes of slope are in agreement with the expected exponential decrease of D, as for the Hamiltonian case (Lega et al. 2003).

As usual, maps are more suited for numerical experiments and the result obtained for the map span almost 2.5 order of magnitude in ϵ while they span only 1.5 order of magnitude in ϵ for the Hamiltonian. It would be natural at this point, at least for the map, to check if the exponential upper bound $D(\epsilon) < \exp -(1/\epsilon)^b$ expected from Nekhoroshev theorem can be obtained from our data, and in particular if one can provide a numerical estimate of b. Indeed, an exponential fit of our data would give the value $b = 0.28$ (Fig. 3, right) with apparently very good correlation coefficient of about 0.99. However, how much this computation is meaningful is a delicate matter: the apparently good correlation coefficient is due mainly to the small interval in ϵ used for the exponential fit (Fig. 3); there are not theoretical predictions to compare to the detected value; numerical studies (Benettin and Fassó 1999) have shown that the exponential upper bounds found by perturbation theories are indeed only upper bounds, while the true exchange of energy among the different degrees of freedom with respect to a perturbing parameter typically follows more complicated functional laws. For these reasons, we think it is necessary in the future to perform more numerical studies of the problem.

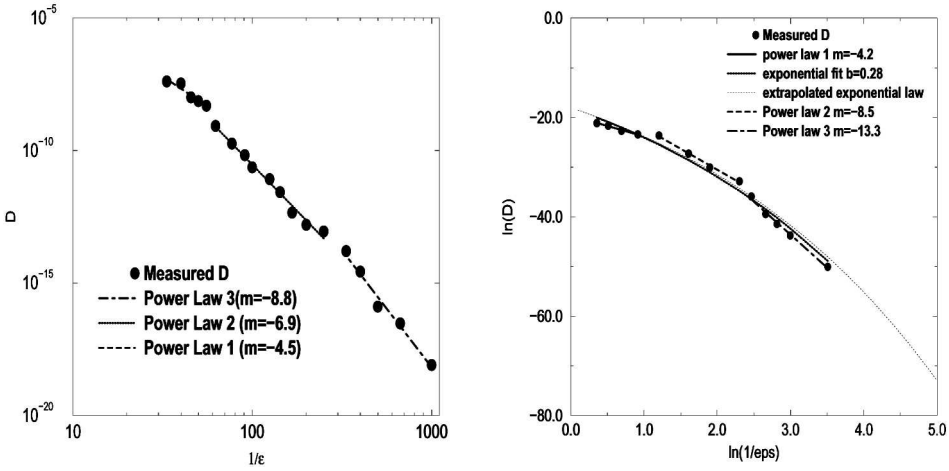

Figure 3: Measure of the diffusion coefficient as a function of $1/\epsilon$. **Left:** For the Hamiltonian model. From Lega et al. 2003. **Right:** for the map. From Froeschlé et al. 2005 The change of slope of the three power law fits is in agreement with the expected exponential decrease of D.

5. 3. GLOBAL ARNOLD'S DIFFUSION

As it is usual, the numerical experiments with maps provide the possibility of exploring the dynamics on much longer integration times with respect to the numerical experiments with the continous flows. Therefore, for a long–term exploration of Arnold diffusion, we focus our attention on the quasi–integrable symplectic map of Eq. 13 studied in Guzzo et al. 2005 for $\epsilon = 0.6$. We have chosen twenty initial conditions near $(I_1, I_2) = (1.71, 0.81)$, i.e. far from resonance crossings and we have computed numerically the map up to 10^{11} iterations.

The results are reported in Fig. 4: on the FLI chart of the action plane (I_1, I_2) we plotted as black dots all points of the orbits which have returned after some time on the section defined by $|\phi_1| \leq 0.005$ and $|\phi_2| \leq 0.005$. Fig. 4a shows only the location of initial conditions (inside the circle), and Fig. 4b shows the result after the intermediate (but already long) time $t = 2.10^9$. Figs. 4c,d show the result after much longer times. To properly display such long term evolutions we needed to use a zoomed out map of the action plane.

In both cases, the orbits filled a macroscopic region of the action plane whose structure is clearly that of the Arnold web. The orbits have moved along the single resonances, and avoided, in many cases, the center of the main resonance crossings, in agreement with the theoretical results of Nekhoroshev 1977 which predict longer stability times for motions in these regions. The larger resonances (which correspond to the smallest orders $|k|$) are practically all visited, while this is not the case for the thinnest ones (which correspond to the highest orders $|k|$). This is in agreement with the theoretical results of Morbidelli and Giorgilli 1995, which predict that the speed of diffusion on each resonance becomes smaller for resonances of high order. Therefore, the possibility of visiting all possible resonances is necessarily limited by finite computational time.

On average, the drift behaves as a diffusion process. In fact, in the case of the map, the average evolution of the squared distance of (I_1, I_2) from the initial datum increases almost linearly with time (Fig. 5), so that we can measure a diffusion coefficient $D \sim 1.7\ 10^{-10}$. The same qualitative behaviour appears when dealing with Hamiltonian (12). The results (Guzzo et al. 2005) are more striking with the map for obvious computational reasons. We remark that this diffusion coefficient characterizes the global diffusion process, while diffusion coefficients measured in Lega et al. 2003 (and reported in the previous Section) characterized local diffusion along a specific resonance.

The described diffusion phenomenon is very different from Chirikov diffusion, where the overlapping of resonances allows diffusion in macroscopic regions of phase space in relatively short time scales and without apparent peculiar topological properties of the stochastic region. For comparison with the Chirikov diffusion regime, in Fig. 6 we plot the evolution of 20 orbits for a high value of ϵ such that the system is in the Chirikov regime.

It is also interesting to remark that the Largest Characteristic Indicator (whose limit for t going to infinity is the largest Lyapunov exponent) computed on two orbits with very close initial conditions (taken at a distance $d = 10^{-4}$) in the Nekhoroshev regime are different (Fig. 7, Froeschlé et al. 2005) and also they do not show clear convergence up to $t = 10^{11}$ iterations. Of course convergence can occur on a much

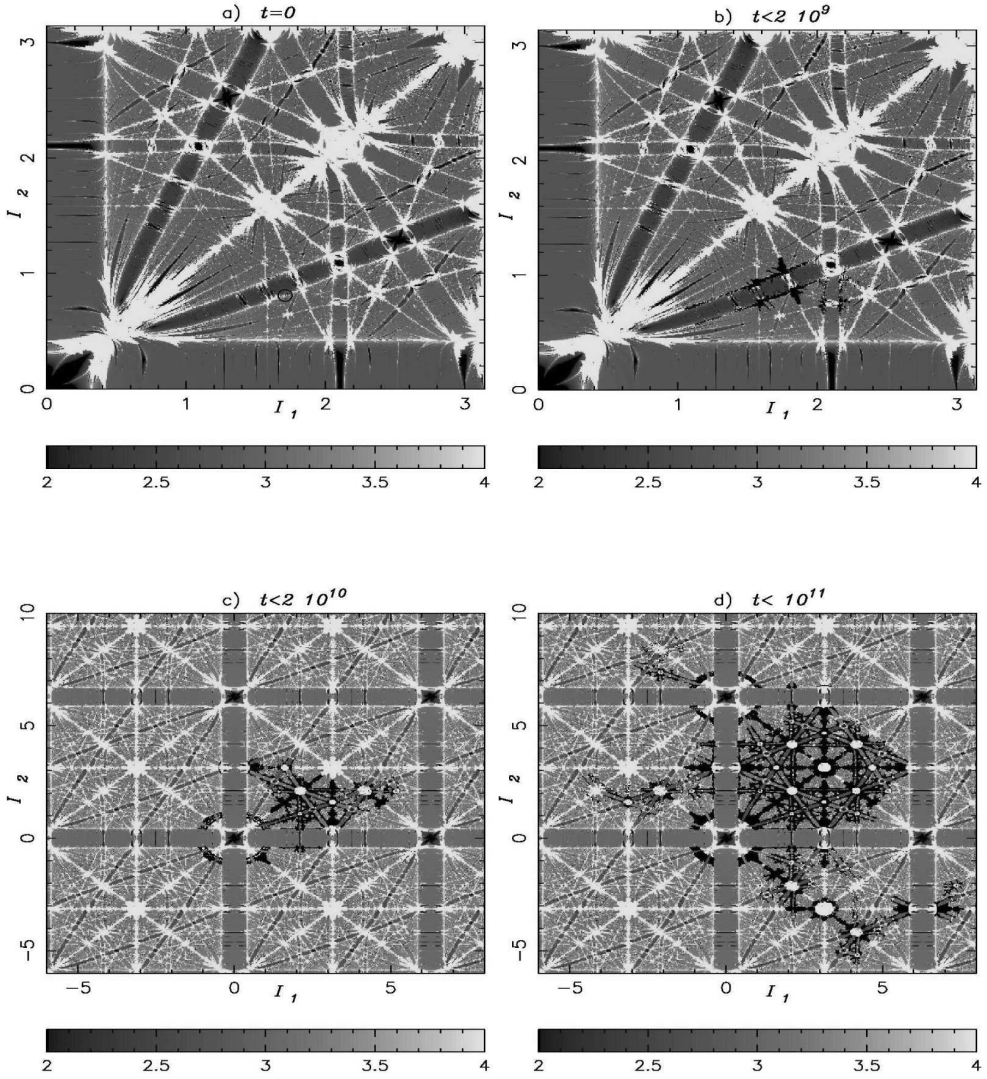

Figure 4: The four panels correspond to the FLI map of the action plane (I_1, I_2) for the map 13, with initial condition on the section S , with different magnifications. The white region corresponds to the chaotic part of the Arnold web. Moreover, on panel (a) we mark with a circle the location of the twenty initial conditions; on panel (b,c,d) we mark with a black dot all points of the twenty orbits which have returned after some time on the section S. We consider $2\,10^9$ iterations for panel (b); $2\,10^{10}$ iterations for panel (c) and 10^{11} iterations for panel (d). From Guzzo et al. 2005.

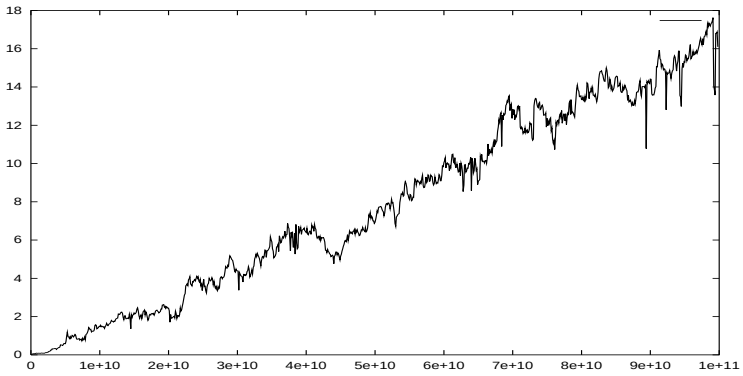

Figure 5: Average evolution of the squared distance of (I_1, I_2) from the initial datum for the map, measured for the points on the section S. The total computation time $t = 10^{11}$ iterations has been divided in 10^3 intervals. For each initial condition, and for each interval $[(n-1)10^8, n10^8]$, we have computed the average of the squared distance of (I_1, I_2) from the initial datum, taking into account only points that in the interval $[(n-1)10^8, n10^8]$ are on the section S. Then, we averaged over all particles. From Guzzo et al. 2005.

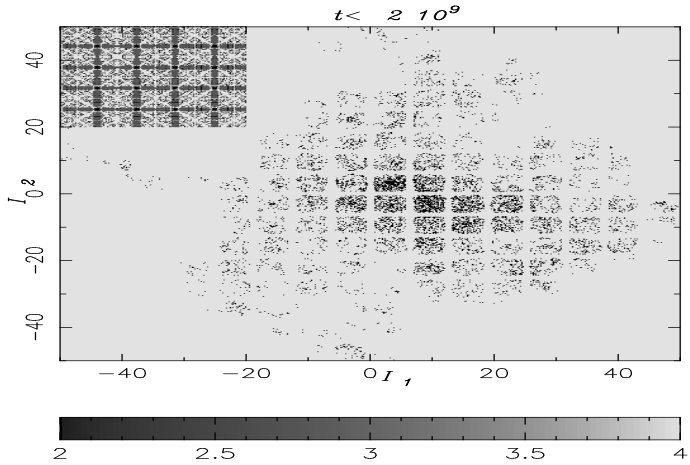

Figure 6: Evolution on section S (black dots) of 20 orbits for the map (2) on a time $t < 210^9$ iterations for $\epsilon = 1.6$. This figure as to be compared with Fig. 4b,c,d showing clearly the fundamental differences between the diffusion of Arnold's type and that of Chirikov type. In the left upper corner we plotted, for reference the FLI map. The white gray corresponds to chaotic orbits. The basic texture of the FLI chart shows that the phase space is almost completely chaotic apart for the regular resonant strips corresponding to $I_1 = 0$ and $I_2 = 0$ and their 2π periodic repetitions. From Guzzo et al. 2005

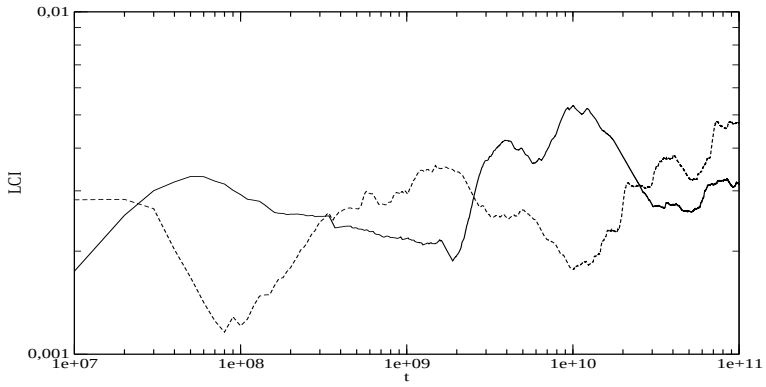

Figure 7: Evolution with time of the Largest Characteristic Indicator of two orbits diffusing on the Arnold web and having close initial conditions (initial distance $\sim 10^{-4}$). From Froeschlé et al. 2005

longer integration time. The same quantity, when computed on a single stochastic region, as it is in the Chirikov regime, converges to the largest Lyapunov Exponent.

References

Arnold, V. I.:1963, Proof of a theorem by A.N. Kolmogorov on the invariance of quasi-periodic motions under small perturbations of the Hamiltonian, *Russ. Math. Surv.*, **18**, 9.

Arnold, V. I.: 1964, Instability of dynamical systems with several degrees of freedom, *Sov. Math. Dokl.*, **6**, 581–585.

Benettin, G. and Fassó, F.: 1999, From Hamiltonian perturbation theory to symplectic integrators and back, *Applied Numerical Mathematics*, **29**, 73-87.

Chirikov, B. V.: 1979, *Phys. Reports*, **52**, 265.

Chirikov, B. V., Ford, J. and Vivaldi, F.: 1979, Some numerical studies of Arnold diffusion in a simple model, Nonlinear Dynamics and the Beam-Beam interaction, M. Month and J.C. Herrera eds., American Institute of Physics.

Delshams, A., De La Llave, R. and Seara, T. M.: 2003, A geometric mechanism for diffusion in Hamiltonian systems overcoming the large gap problem: Announcement of results, *ERA Amer. Math. Soc.*, **9**, pp. 125–134.

Efthymiopoulos, C., Voglis, N. and Contopoulos, G.: 1998, Diffusion and transient spectra in a 4-dimensional symplectic map, in: Analysis and Modeling of Discrete Dynamical Systems, Advances in Discrete mathematics and Applications, Eds. Benest D. and Froeschlé C.

Froeschlé, C. and Scheidecker, J. P.: 1973, On the disappearance of isolating integrals in systems with more than two degrees of freedom, *Astrophys. and Space Sc.*, **25**, pp. 373-386.

Froeschlé, C., Guzzo, M. and Lega, E.: 2000, Graphical evolution of the Arnold's web: from order to chaos, *Science*, **289**, N.5487, pp. 2108–2110.

Froeschlé, C., Guzzo, M. and Lega, E.: 2005, Local and global diffusion along resonant lines in discrete quasi–integrable dynamical systems, *Cel. Mech and Dynam. Astron.*, **92**, pp. 243-255.

Froeschlé, C., Lega, E. and Gonczi, R.: 1997, Fast Lyapunov indicators. Application to asteroidal motion, *Celest. Mech. and Dynam. Astron.*, **67**, pp. 41–62.

Giordano and Cincotta: 2004, Chaotic diffusion of orbits in systems with divided phase-space, *Astron. Astrophys.*, **423**, pp. 745–753.

Guzzo, M. and Benettin, G.: 2001, A spectral formulation of the Nekhoroshev theorem and its relevance for numerical and experimental data analysis, *DCDS B*, **1**, 1-28.

Guzzo, M., Lega, E. and Froeschlé, C.: 2002, On the numerical detection of the effective stability of chaotic motions in quasi–integrable systems, *Physica D*, **163**, pp. 1–25.

Guzzo, M., Lega, E. and Froeschlé, C.: 2005, First numerical evidence of global Arnold diffusion in quasi–integrable systems, *DCDS-B*, **5**, pp. 687–698.

Guzzo, M., Lega, E. and Froeschlé, C.: 2006, Diffusion and stability in perturbed non-convex integrable systems, *Nonlinearity*, **19**, pp. 1049–1067.

Guzzo, M.: 2004, A direct proof of the Nekhoroshev theorem for nearly integrable symplectic maps, *Annales Henry Poincaré*, **5**, 1013-1039.

Guzzo, M.: 2005, The web of three-planet resonances in the outer Solar System, *Icarus*, **174**, 273-284.

Kolmogorov, A. N.: 1954, On the conservation of conditionally periodic motions under small perturbation of the Hamiltonian, *Dokl. Akad. Nauk. SSSR*, **98**, 524.

Laskar, J.: 1993, Frequency analysis for multi-dimensional systems. Global dynamics and diffusion, *Physica D*, **67**, pp. 257–281.

Lega, E., Guzzo, M. and Froeschlé, C.: 2003, Detection of Arnold diffusion in Hamiltonian systems, *Physica D*, **182**, pp. 179–187.

Lichtenberg, A. J. and Aswani, A. M.: 1998, Arnold diffusion in many weakly coupled maps, *Physical Review E*, **57**, pp. 5325-5331.

Lichtenberg, A. J. and Lieberman, M. A.: 1983, Regular and Chaotic Dynamics, Springer-Verlag.

Lega, E., Froeschlé, C. and Guzzo, M.: 2007, "Diffusion in Hamiltonian quasi-integrable systems", in Topics in Gravitational Dynamics, Lecture Notes in Physics 729, D. Benest, C. Froeschlé and E. Lega eds., 29-65.

Moser, J.: 1958, On invariant curves of area-preserving maps of an annulus, *Comm. on Pure and Appl. Math.*, **11**, 81–114.

Morbidelli, A.: 2002, Modern Celestial Mechanics, Advances in Astronomy and Astrophysics, Taylor and Francis.

Morbidelli, A. and Giorgilli, A.: 1995, On a connection between KAM and Nekhoroshev's theorems, *Physica D*, **86**, 514–516.

Nekhoroshev, N. N.: 1977, Exponential estimates of the stability time of near-integrable Hamiltonian systems, *Russ. Math. Surveys*, **32**, 1–65.

Tennyson, J. L., Lieberman, M. A., Lichtenberg, A. J.: 1979, Diffusion in near-integrable Hamiltonian systems with three degrees of freedom, Nonlinear Dynamics and the Beam-Beam interaction, M. Month and J.C. Herrera eds., American Institute of Physics.

Kuksin, S. B.: 1993, On the inclusion of an almost integrable analytic symplectomorphism into a Hamiltonian flow. *Russian Journal of Math. Phys.*, **1**, pp. 191–207

Kuksin, S. B. and Pöschel, J.: 1994, On the inclusion of analytic symplectic maps in analytic Hamiltonian flows and its applications, *Nonlinear Differential Equations Appl.*, **12**, pp. 96–116.

Wood, B. P., Lichtenberg, A. J. and Lieberman, M. A.: 1990, Arnold diffusion in weakly coupled standard map, *Phys. Rev. A*, **42**, pp. 58 85-5893.